

High-Order Methods for Turbulent Flow Simulations on Deforming Domains

Per-Olof Persson

Department of Mathematics, University of California, Berkeley
Mathematics Department, Lawrence Berkeley National Laboratory

Joint work with B. Froehle, L. Wang, S. Kanner, M. Fortunato,
M. Zahr, D. J. Willis, S. Govindjee, J. Peraire, X. Roca, G. Dahlbacka

Antony Jameson 80th Birthday Symposium
Stanford University

High-Order Discontinuous Galerkin Simulations

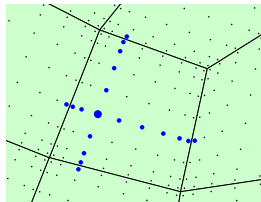
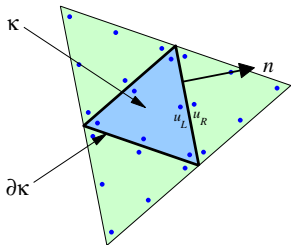
- Discontinuous Galerkin (DG) methods have desirable properties:

	FVM	FDM	FEM	DG
1) High-order/Low dispersion	✗	✓	✓	✓
2) Complex geometries	✓	✗	✓	✓
3) Stability for conservation laws	✓	✓	✗	✓

- However, several problems to resolve:
 - High CPU/memory requirements (compared to FVM or H-O FDM)
 - Robustness issues, low tolerance to under-resolved features
 - High-order geometry representation and mesh generation
- Need to make DG competitive for real-world problems*

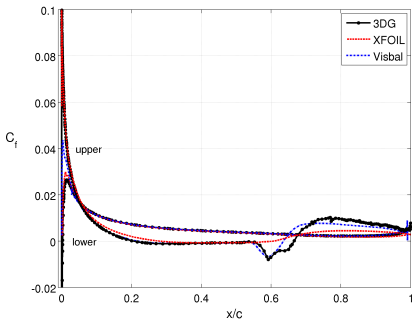
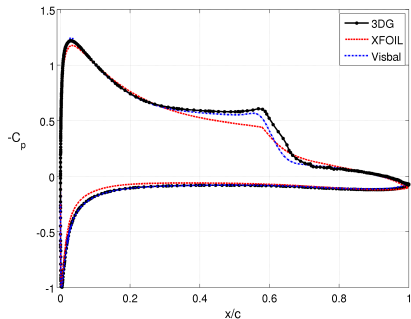
The 3DG Software Package

- Standard nodal high-order DG discretization for conservation laws
- Curved, fully unstructured meshes of tetrahedra/hexahedra
- General multiphysics formulation – same code used for fluid/structure, for DG/CG, etc, with modular interfaces
- Fully implicit formulation, sparse block formats for Jacobians
- Highly sparse “Line-DG” formulation for quad/hex elements
- Efficient parallel solvers with matrix-based decompositions– nearly perfect speedup to 10,000’s of cores for time-accurate problems



Example: ILES at $Re = 60,000$

- Implicit LES for flow past airfoil [Uranga *et al* 2009, 2011]
- Separation and transition well captured
- Good agreement with XFOIL and previously published ILES



Average pressure and skin friction coefficients

Computational Domain

2D and 3D NACA0012 Airfoil for $0^\circ \leq \alpha \leq 90^\circ$

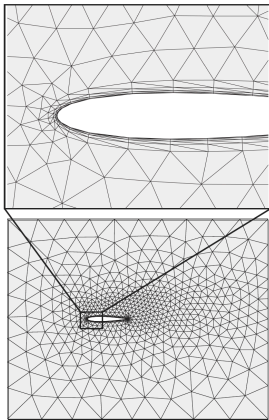


Figure: Mesh 0 (2D)

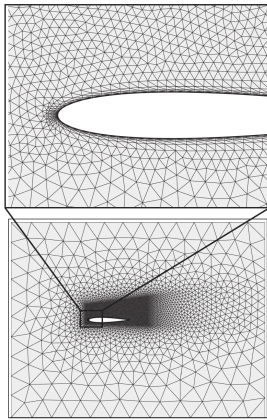


Figure: Mesh 2 (2D)

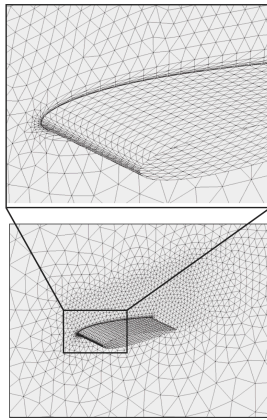


Figure: Mesh 1 (3D)

Flow Structure, single NACA Airfoil at $Re=5.3k$

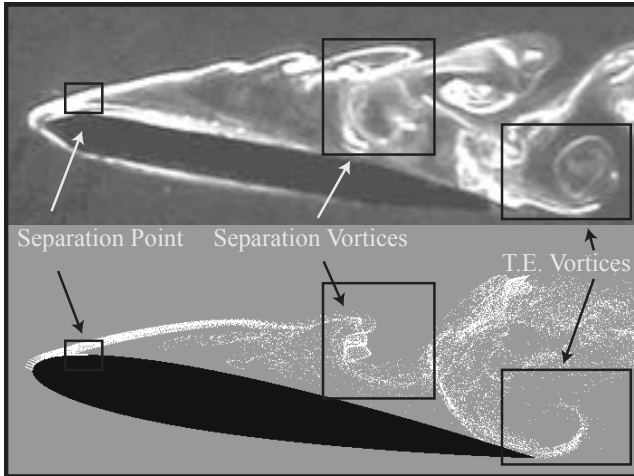


Figure: Comparison of flow structure to LIF visualization

Forces, single NACA Airfoil at Low Re

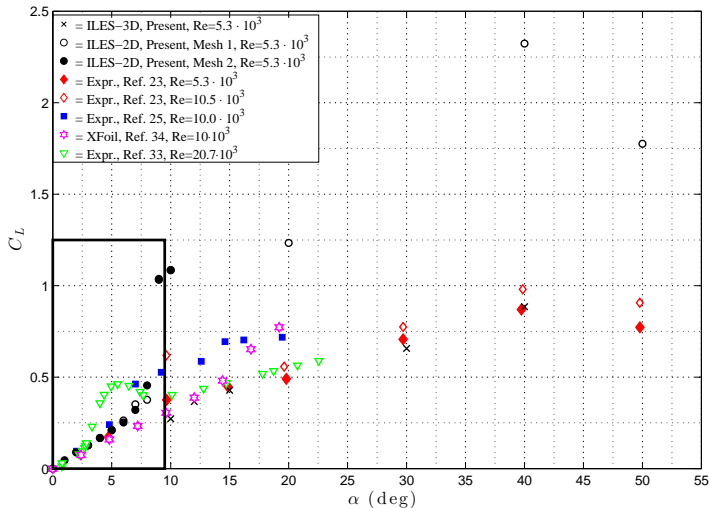


Figure: Lift Coefficient for $0^\circ \leq \alpha \leq 55^\circ$ with $5,000 \leq Re \leq 21,000$

Forces, single NACA Airfoil at $Re=40k$

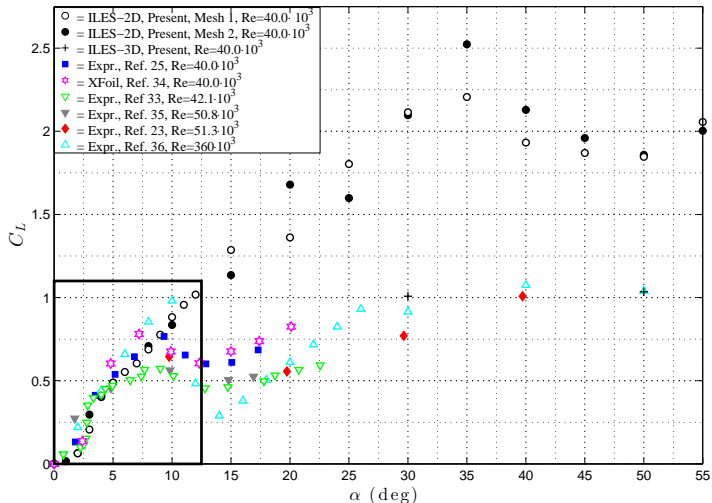


Figure: Lift Coefficient for $0^\circ \leq \alpha \leq 55^\circ$ with $Re \geq 40,000$

Frequency content of forces

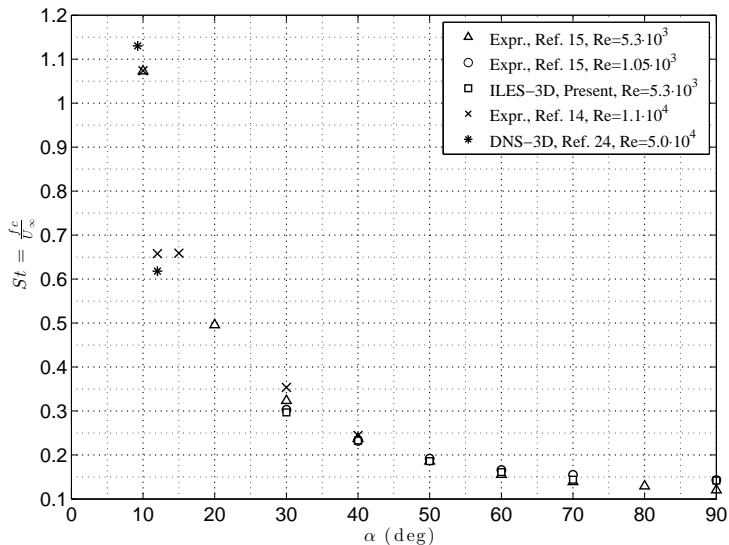
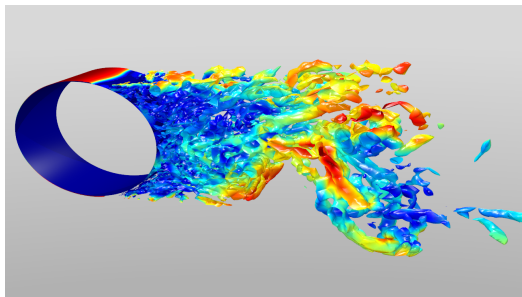
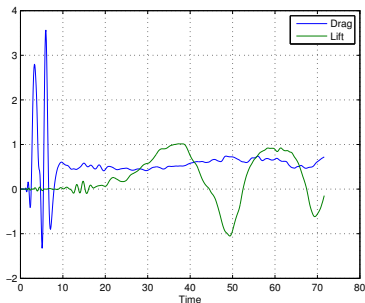


Figure: Frequency content of lift force at $Re=5.3 \cdot 10^3$ (Expr from Alam, 2011).

Cylinder – Delayed Detached Eddy Simulation

- DES/DDES [Spalart 1997,2006]: Hybrid RANS/LES model for problems with significant flow separation
- Edge of boundary layer moving; stabilize by continuous AV
- Model problem: Flow over cylinder, $Re = 1.5 \cdot 10^6$
- Left: Force coefficients C_D, C_L , Right: Q-criterion isosurfaces



ALE Formulation for Deforming Domains

- Use mapping-based ALE formulation for moving domains
[Visbal,Gaitonde 2002], [Persson,Bonet,Peraire 2009]
- Map from reference domain V to physical deformable domain $v(t)$
- Introduce the *mapping deformation gradient* $\mathbf{G} = \nabla_X \mathcal{G}$ and the *mapping velocity* $\mathbf{v}_X = \frac{\partial \mathcal{G}}{\partial t} \Big|_X$, and set $g = \det(\mathbf{G})$
- For numerically computed grid motions, compute *stage consistent* velocities by imposing

$$\mathbf{x}_i = \mathbf{x}_0 + \Delta t \sum_{j=1}^s a_{ij} \mathbf{v}_j \quad \Longrightarrow \quad \mathbf{v}_i = \sum_{j=1}^s (A^{-1})_{ij} \frac{\mathbf{x}_j - \mathbf{x}_0}{\Delta t}, \quad i = 1, \dots, s,$$

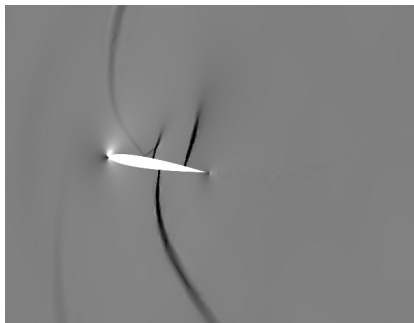
where A is the implicit Runge-Kutta Butcher tableaux

[Froehle & Persson, in review]

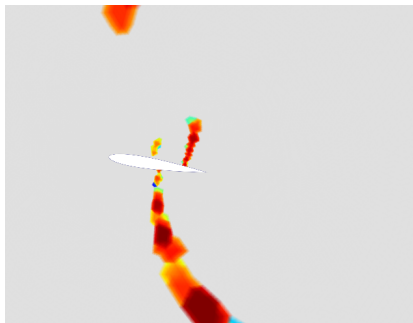
- Transform equations to account for the motion

Pitching wing in transonic flow

- ALE formulation for the Euler equations combined with sensor-based artificial diffusion
- Freestream $Ma = 0.6$, AoA harmonic with amplitude = 30°
- Implicit solver, re-used Jacobians



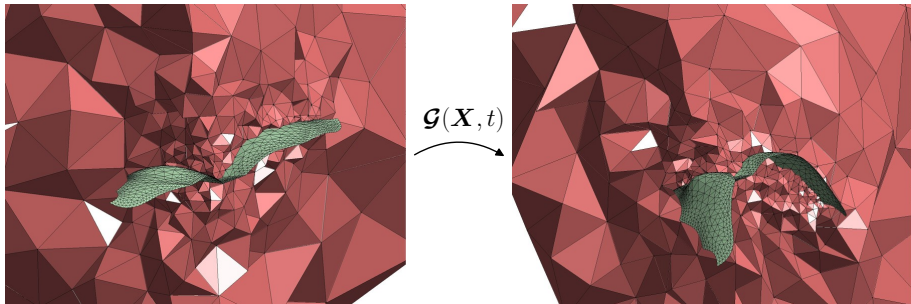
x -gradient of density



Artificial viscosity

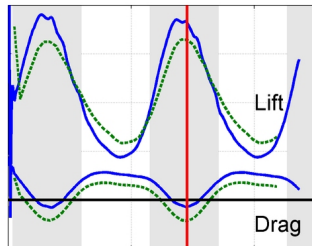
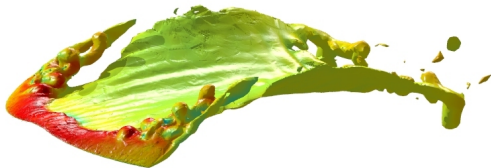
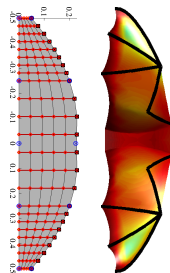
Nonlinear Elasticity for Deforming Domains

- Non-linear solid mechanics approach used to deform meshes
- High-order ALE methods require a smooth mapping $\mathcal{G}(X, t)$ such that the elements are aligned with the moving boundaries
- Example: Flapping bat wings, wing motion from experimental data
- A reference mesh (left) is deformed elastically (right)



Optimal Flapping Kinematics

- **Goal:** To design and analyze an effective flapping wing shape for cruising flight
- *A multi-fidelity approach* with a range of simulation tools [Willis & Persson 2011, 2014]



Vertical Axis Wind Turbines

- Recent interest in vertical axis wind turbines (VAWT):
 - 2D airfoils, easy to manufacture, supportable at both ends
 - Omnidirectional (good in gusty, low wind, e.g. close to ground)
 - Lower blade speeds – lower noise and impact
 - Can be packed close together in wind farms
- Numerical simulations can help overcome remaining challenges:
 - Lower theoretical (and practical) efficiency than HAWTs
 - Sensitive to design conditions
 - Structural problems, fatigue and catastrophic failure



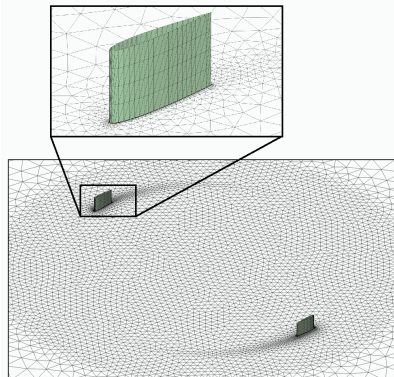
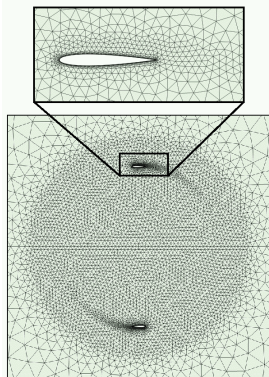
(3kW unit, G. Dahlbacka, LBNL)

VAWT – Mathematical Model and Discretization

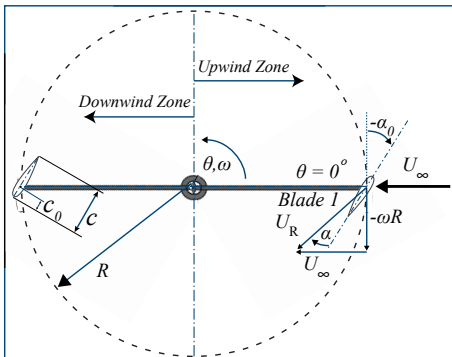
- Solve the Navier-Stokes equations in a rotating frame:

$$\mathcal{G}(X, Y, t) = \begin{bmatrix} \cos \omega t & -\sin \omega t \\ \sin \omega t & \cos \omega t \end{bmatrix} \begin{bmatrix} X \\ Y \end{bmatrix}$$

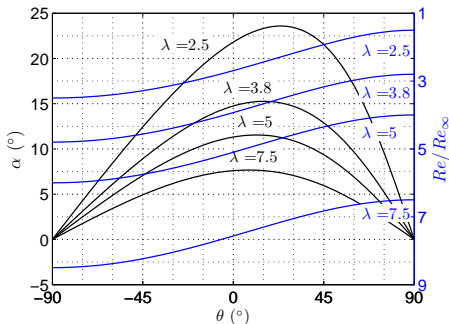
- Hybrid boundary layer/unstructured mesh, element degree $p = 3$



Range of angle-of-attack (α) based on TSR (λ)



Bird's-eye-view of 2-bladed VAWT

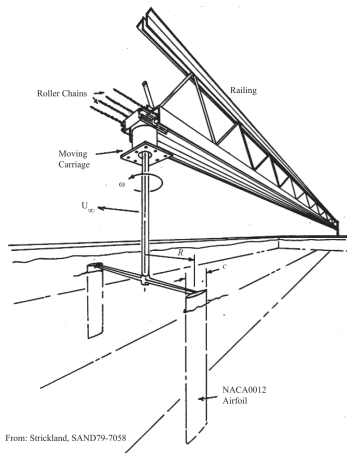


Variation of angle-of-attack at various TSR as a function of azimuthal angle

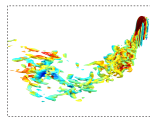
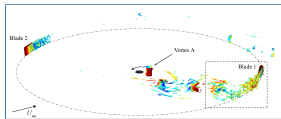
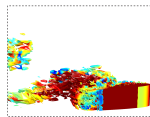
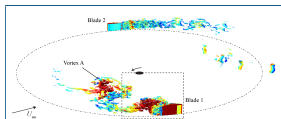
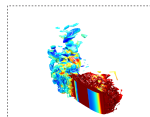
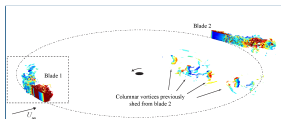
$$\lambda = \frac{\omega R}{U_{\infty}}$$

Sandia National Laboratories' Low Re VAWT

Sandia National Labs tow tank experiment from 1979

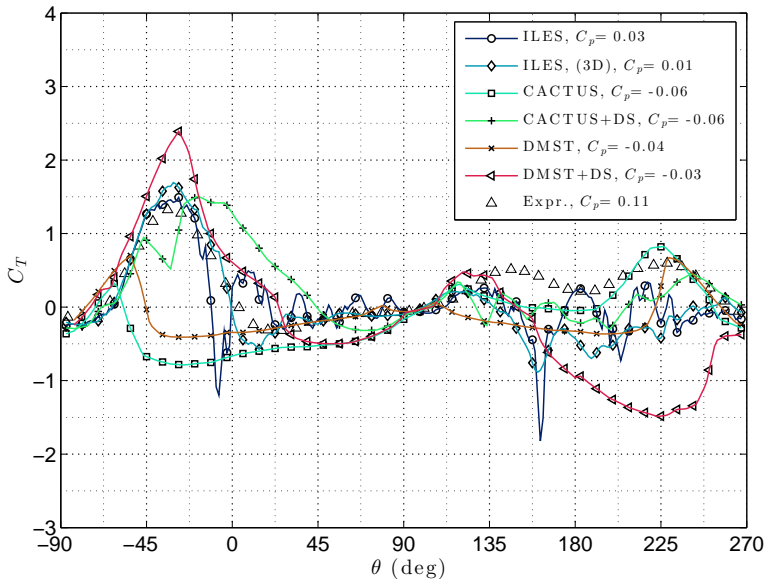


From: Strickland, SAND79-7058



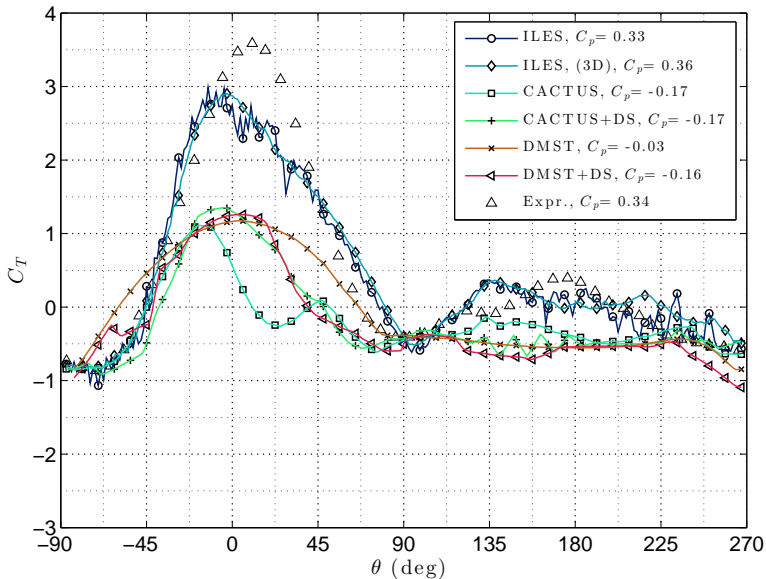
Results of SNL VAWT Simulations

ILES vs Analytical Models vs Experiments, $\lambda=2.5$



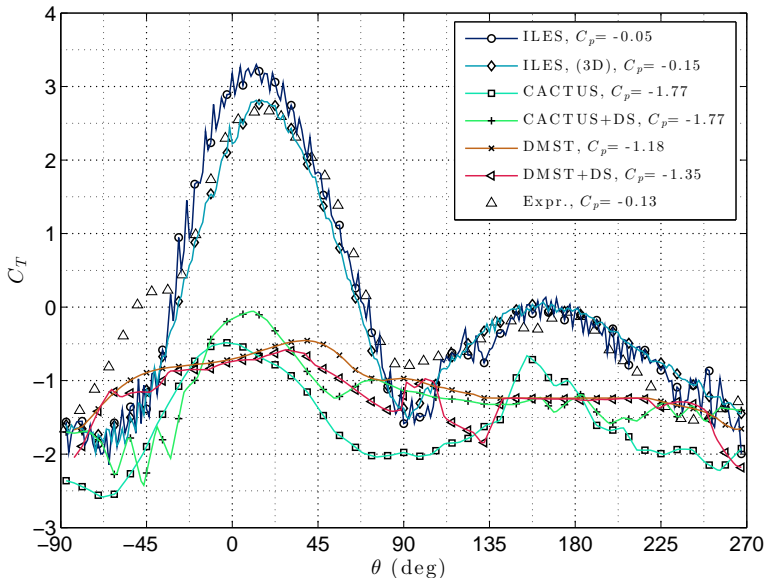
Results of SNL VAWT Simulations

ILES vs Analytical Models vs Experiments, $\lambda=5.0$



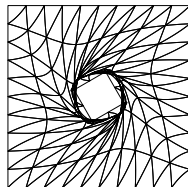
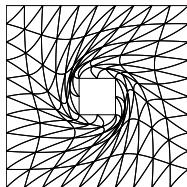
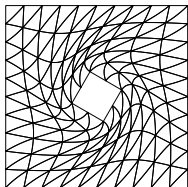
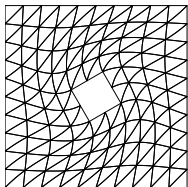
Results of SNL VAWT Simulations

ILES vs Analytical Models vs Experiments,

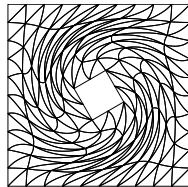
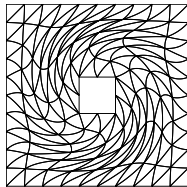
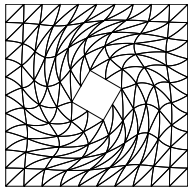
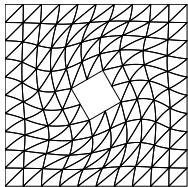


Domains with Large Deformations

- For large deformations, it is in general not possible to deform the meshes smoothly – *remeshing required*
- For efficient numerical schemes, use *local* mesh operations



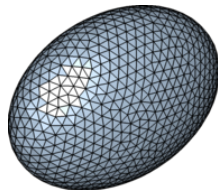
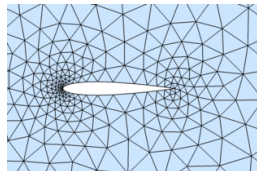
Radial basis functions



Nonlinear elasticity

The DistMesh Mesh Generator

- High quality meshes obtained using the *DistMesh* algorithm [Persson, Ph.D. thesis, 2005]
 1. Start with *any* topologically correct initial mesh
 2. Move nodes to find force equilibrium in edges
 - Project boundary nodes using *implicit geometry* $\phi(\mathbf{x})$
 - Update element connectivities with Delaunay
- Excellent properties:
 - Very simple (1 page of MATLAB)
 - Implicit geometries → No CAD required
 - Very high element qualities
 - Moving meshes/deforming domains
- Widely used:
 - Numerous books and courses
 - Rewritten in C, C++, C#, Fortran 77/90, Python, Mathematica, Octave



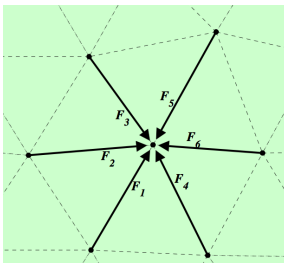
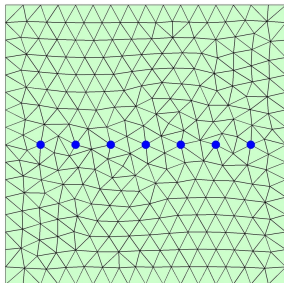
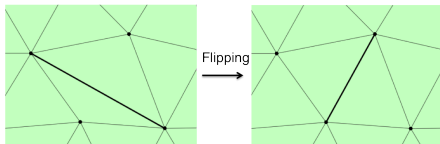
Mesh Motion and Edge Flipping

- Move the boundary nodes according to the prescribed geometry motion.
- Iteratively update the positions of interior nodes driven by spring-based force.

$$\mathbf{p}^{(n+1)} = \mathbf{p}^{(n)} + \delta \sum_i \mathbf{F}_i$$

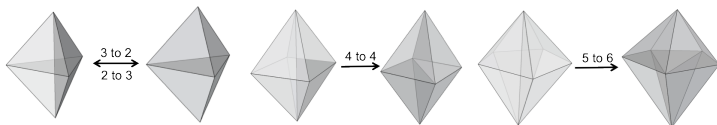
$$|\mathbf{F}_i(l)| = \begin{cases} k(l - l_0) & \text{if } l \geq l_0, \\ 0 & \text{if } l < l_0, \end{cases}$$

- Edge Flipping. Each element can be flipped once during each time step

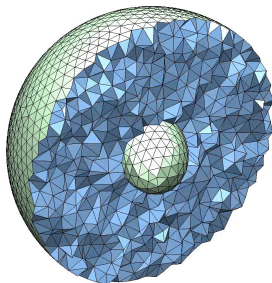
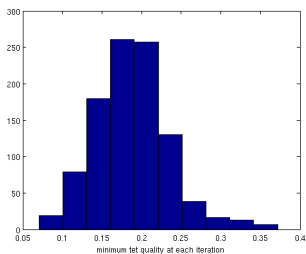


Element flipping in 3-D

- Local flipping in the 3D case:

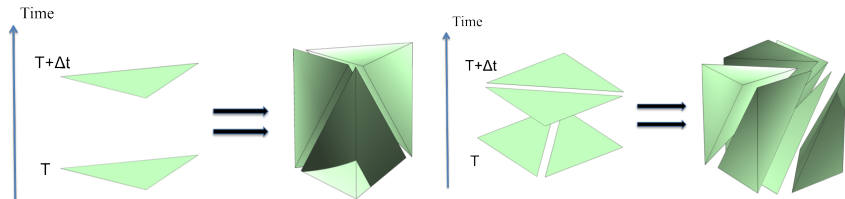


- The local flipping operations restrict the topology changes within a small number of elements



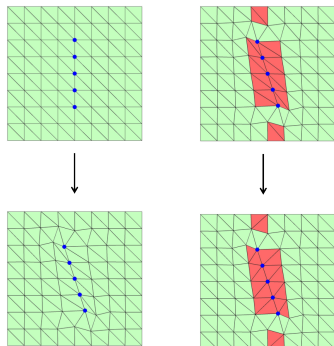
Time-stepping with topology changes

- Various approaches for high-order time-stepping with element flips
- Fully unstructured space-time DG method: [Wang/Persson 2013]
 - Fully consistent discretization in both space and time
 - Allows for arbitrary mesh deformations and topology changes
 - Local mesh operations significantly simplify the process of space-time slab mesh generation



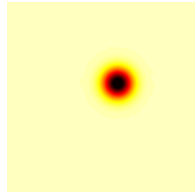
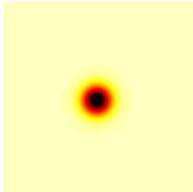
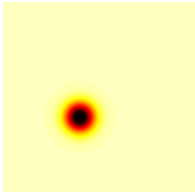
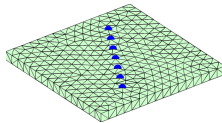
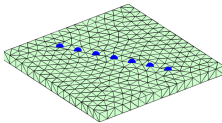
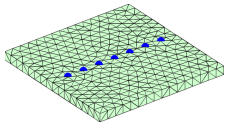
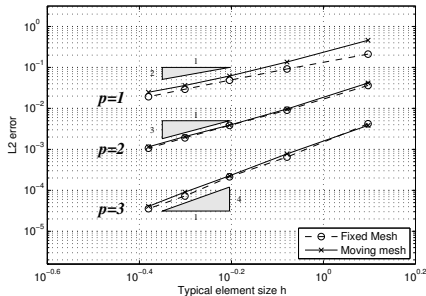
Time-stepping with topology changes

- Combination of the ALE formulation and local L^2 projections
 - For general re-meshing, this typically introduces significant errors and the implementation is complicated for general 3-D meshes
 - Instead, move nodes using the ALE formulation and apply local L^2 projections within each pair of red cells:

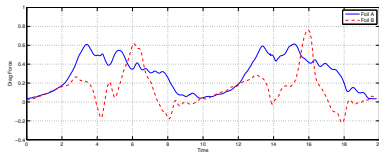
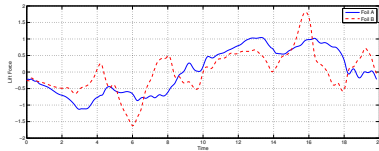
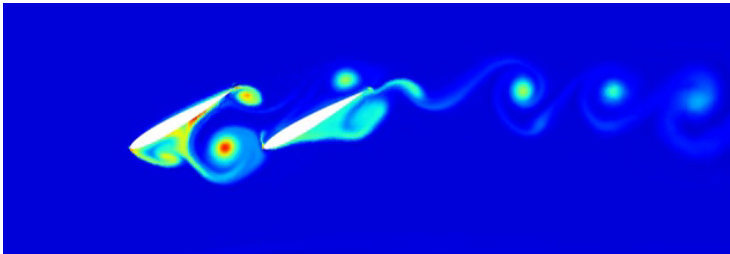


Example: Euler Vortex, Convergence

- Propagate an Euler Vortex on a fixed domain but moving mesh
- Optimal order of convergence $O(h^{p+1})$ for fixed and moving mesh.



Example: Tandem Foils



Current work: Double VAWT Simulation

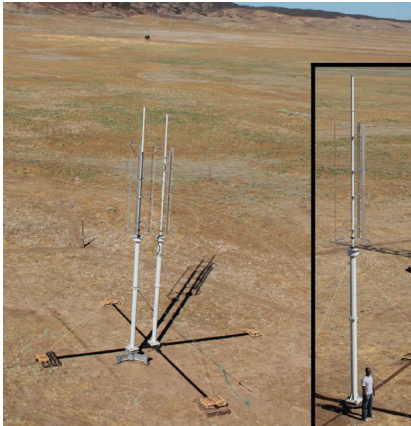


Figure: Counter-rotating VAWT experimental test site in the Antelope Valley, LA County, CA. (From Dabiri, 2011).

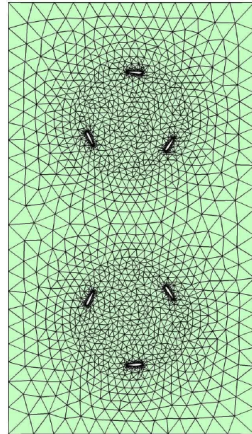


Figure: Computational domain for double VAWT simulation

Conclusion

- High-order LES with moving boundaries
- Moving mesh technique based on local mesh operations
- Applications in DNS/LES/DDES flow problems, flapping flight, wind turbine simulations, fluid-structure interaction, aeroacoustics